

Lithium and rotation in F and G dwarfs and subgiants^{*}

Sushma V. Mallik, M. Parthasarathy, and A. K. Pati

Indian Institute of Astrophysics, Bangalore 560034, India

Received 16 April 2003 / Accepted 4 July 2003

Abstract. Lithium abundances have been determined in 127 F and G Pop I stars based on new measurements of the equivalent width of the $\lambda 6707$ Å Li I line from their high resolution CCD spectra. Distances and absolute magnitudes of these stars have been obtained from the Hipparcos Catalogue and their masses and ages derived, enabling us to investigate the behaviour of lithium as a function of these parameters. Based on their location on the HR diagram superposed on theoretical evolutionary tracks, the sample of the stars has been chosen to ensure that they have more or less completed their Li depletion on the main sequence. A large spread in the Li abundances is found at any given effective temperature especially in the already spun down late F and early G stars. This spread persists even if the “Li-dip” stars that have evolved from the main sequence temperature interval 6500–6800 K are excluded. Stars in the mass range up to $2 M_{\odot}$ when divided into three metallicity groups show a linear correlation between Li abundance and mass, albeit with a large dispersion around it which is not fully accounted for by age either. The large depletions and the observed spread in Li are in contrast to the predictions of the standard stellar model calculations and suggest that they are aided by non-standard processes depending upon variables besides mass, age and metallicity. The present study was undertaken to examine, in particular, the effects of rotation on the depletion of Li. No one-to-one correlation is found between the Li abundance and the present projected rotational velocity. Instead the observed abundances seem to be dictated by the rotational history of the star. However, it is noted that even this interpretation is subject to the inherent limitation in the measurement of the observed Li EQW for large rotational velocities.

Key words. stars: abundances – stars: late-type – stars: rotation

1. Introduction

Old Pop. II stars are observed to have ${}^7\text{Li}$ abundances up to $\log N(\text{Li}) \sim 2.1$ and young, Pop. I stars up to a maximum of ~ 3.3 (on the scale of $\log N(\text{H}) = 12.0$) which is inferred to be the current Galactic ${}^7\text{Li}$ abundance, the abundance these stars are believed to have inherited at birth. Lithium is one of the most fragile elements, burning at only a few million degrees ($\geq 2.5 \times 10^6$ K) through the reaction ${}^7\text{Li}(p, \alpha){}^4\text{He}$. In a typical main sequence (MS) star, the outer 2–3% of the stellar mass is cooler than the Li-burning temperature and thus Li survives only in this region. This comprises about 40% of the stellar radius, the so called Li-preservation zone and inside of it is the Li-depleted region. The standard stellar models do not predict MS depletion of Li in any except the coolest dwarfs ($T_{\text{eff}} < 4000$ K) because the bottom of the convection zone (which is about 10% of the stellar radius) remains cooler than the Li-burning temperature. There have been several observations in the past of Li in main sequence stars

of $T_{\text{eff}} > 5800$ K and over a large range of metallicity (Rebolo et al. 1988; Lambert et al. 1991 and most recently Chen et al. 2001) which suggest enrichment of the Galaxy in Li from ~ 2.0 at $[\text{Fe}/\text{H}] \leq -1.4$ through ~ 2.4 at $[\text{Fe}/\text{H}] = 0.5$ to ~ 3.3 at $[\text{Fe}/\text{H}] \sim +0.2$. The striking result of these studies is the progressive increase of dispersion in Li for higher metallicities. In particular, there is an enormous variation of more than 3 dex in the metallicity range $[\text{Fe}/\text{H}] \sim 0.0$. A study of 200 old disk-population F stars by Balachandran (1990) showed a large scatter in their Li abundance strongly indicating that Li depletion must be occurring on the main sequence. In fact, enough observational evidence exists now to suggest that a vast majority of field F and early G dwarfs and subgiants deplete their surface Li often quite severely (Herbig 1965; Duncan 1981; Pallavicini et al. 1987; Randich et al. 1994, 1995, 1999; Pasquini et al. 1994, 1997; de Medeiros et al. 1997; Lebre et al. 1999). That Li depletion takes place on the MS itself has now been amply evidenced by comparison between G dwarfs in the Pleiades (Soderblom et al. 1993a) and the Hyades (Thorburn et al. 1993) clusters where the older Hyades stars have less Li than the Pleiades stars at the same effective temperature. Over the past 15 years, an increasingly large body of data have accumulated on other clusters of different ages and metallicities, e.g. α Persei (Balachandran et al. 1988, 1996),

Send offprint requests to: S. V. Mallik,
e-mail: sgvmk@iiap.ernet.in

^{*} Table 1 is only available in electronic form at the CDS via anonymous ftp to cdsarc.u-strasbg.fr (130.79.128.5) or via <http://cdsweb.u-strasbg.fr/cgi-bin/qcat?J/A+A/409/251>

M 34 (Jones et al. 1997), Praesepe (Soderblom et al. 1993b), NGC 752 (Deliyannis et al. 2000), M 67 (Balachandran 1995; Deliyannis 2000; Pasquini et al. 1997). Relative depletion between various clusters and the spread persistent within a given cluster further strengthen the conclusion that there has to be a parameter besides mass, age and metallicity that controls the behaviour of Li (read Jefferies 2000 for a recent review).

The standard stellar model calculations which include only convective mixing and ignore possible effects due to rotation, diffusion, mass loss, magnetic fields and so on fail to explain the observed Pop I Li abundance patterns (Deliyannis et al. 2000). The most striking example is the Li gap in F stars, the so-called Boesgaard-Tripicco dip, a sharp drop in Li of over a factor of 30 in a narrow range in effective temperature between 6500–6800 K first detected by Boesgaard & Tripicco (1986) in the Hyades. This dip is absent in the Pleiades but has been seen in a large number of clusters of ages 200 Myr and more and also in field stars. It once again implies Li depletion is a main sequence phenomenon. The underlying lithium morphology that abundances decrease with age and towards later spectral types do suggest that depletion is basically governed by the deepening convective zone. However, as the base of the surface convection zone especially in F and G stars is not hot and deep enough to destroy Li, this depletion requires surface material to be mixed to hotter temperatures below the convection zone. Such mixing is not predicted by the standard stellar models and it has been a long-standing problem to understand precisely the viable alternative processes that might trigger the mixing and that are not at odds with existing observations.

Several non-standard mixing processes have been invoked to account for Li depletion/dilution in the MS stars. In particular, the non-standard rotational models of Pinsonneault et al. (1989, 1990), Charbonnel et al. (1994) have attempted to explain the depletion of Li by linking it to the process of the transport and dissipation of angular momentum. Stars arrive on the MS rotating rapidly. They undergo a spin-down while on the MS. The rotational models suggest that the outer layers of a star are spun down first due to winds from the surface, leaving the star in a state of differential rotation with angular velocities increasing with decreasing radius. The turbulence generated by the shear forces triggers mixing in the deeper layers causing Li depletion. These models have predicted that a spread in Li abundance will become apparent when stars with a range in initial angular momenta are spun down to approximately the same final rotational velocity; a star with a larger initial angular momentum will undergo a greater amount of rotational spin-down, a larger amount of mixing and thus a larger Li depletion (Pinsonneault et al. 1990).

In order to verify and extend the findings of Balachandran (1990) and Chen et al. (2001), we have obtained new observations of the Li I line at 6707.78 Å in 127 Pop. I stars. The goal of the present study is to particularly investigate if mixing induced by differential rotation as suggested by the above models could in any way explain Li depletion observed in stars otherwise similar. This survey has taken advantage of the knowledge of distances and absolute magnitudes from the Hipparcos Catalogue (ESA, 1997) for all the stars. This has

enabled us to plot thus a large homogeneous sample of stars on the HR diagram superposed on the evolutionary tracks for different masses and actually trace the evolution of Li abundance of a star with respect to its age, mass and rotation. The sample of stars has been selected on the basis that they are slightly evolved off the MS, ensuring that they have completed their Li depletion on the MS and at the same time not evolved far enough towards the red giant branch for their convective envelopes to have deepened and caused significant mixing.

2. Observations and analysis

A large sample of F and G dwarfs and subgiants was selected based on their spectral classification from the Bright Star Catalogue (Hoffleit & Jaschek 1982), the [Fe/H] Catalogue of Cayrel de Strobel et al. (1997) and the Catalogue of Rotational and Radial velocities for evolved stars (de Medeiros & Mayor 1999) and plotted on the HR diagram against the backdrop of theoretical evolutionary tracks due to Girardi et al. (2000) for a typical Pop. I composition. This exercise was done to see exactly what stage of evolution they lie in. The spectral classification is often erroneous as we discover on the HR diagram. Several subgiants actually already on their way up the red giant branch and similarly quite a few giants are still on the left end of the subgiant branch. A sample of 127 stars was selected out of these based on their location on the HR diagram consistent from the point of view of Li evolution in the sense that they have more or less completed their depletion on the MS and have not evolved far enough to undergo dilution on RGB. These stars span a range in [Fe/H] from -0.85 to $+0.72$ and in T_{eff} from 5200 to 7000 K which maximizes their range in $v \sin i$.

Table 1 lists the relevant stellar parameters for the 127 program stars. Columns 2 and 3 give the spectral type and $B - V$ of the star, obtained from the Bright Star Catalogue and the [Fe/H] Catalogue. $\log g$ and [Fe/H] listed in Cols. 5 and 6 have been taken from the [Fe/H] Catalogue and the microturbulent velocity ξ_t in Col. 7 (in units of km s^{-1} from the individual sources for each star listed at the end of the same catalogue. $v \sin i$ for most of the stars is from de Medeiros & Mayor (1999) determined with high precision with the CORAVEL spectrometer (accuracy $\leq 1.0 \text{ km s}^{-1}$) and the rest have been adopted from the Bright Star Catalogue. These are tabulated in Col. 8.

The CCD spectra of these stars have been obtained in the region of the Li I line at 6707.8 Å at a spectral resolution of $\sim 0.35 \text{ Å}$ using the coude echelle spectrograph at the 102 cm telescope at the Vainu Bappu Observatory at Kavalur. The data have been reduced using the IRAF software following exactly the same procedure as described in Mallik (1998). The normalised spectra of 4 sample stars in the neighbourhood of the Li I line are displayed in Fig. 1. The spectra are centred around the 6707.8 Å line and include several Fe I lines that were also used for the wavelength calibration. The Li feature is blended with an Fe I line at 6707.445 Å which was corrected for following the procedure described in detail in Mallik (1998). The observed spectra in the Li I region include 6 other Fe I lines at $\lambda\lambda 6705.105, 6713.044, 6715.386, 6726.673, 6733.153$ and 6752.716 having the same

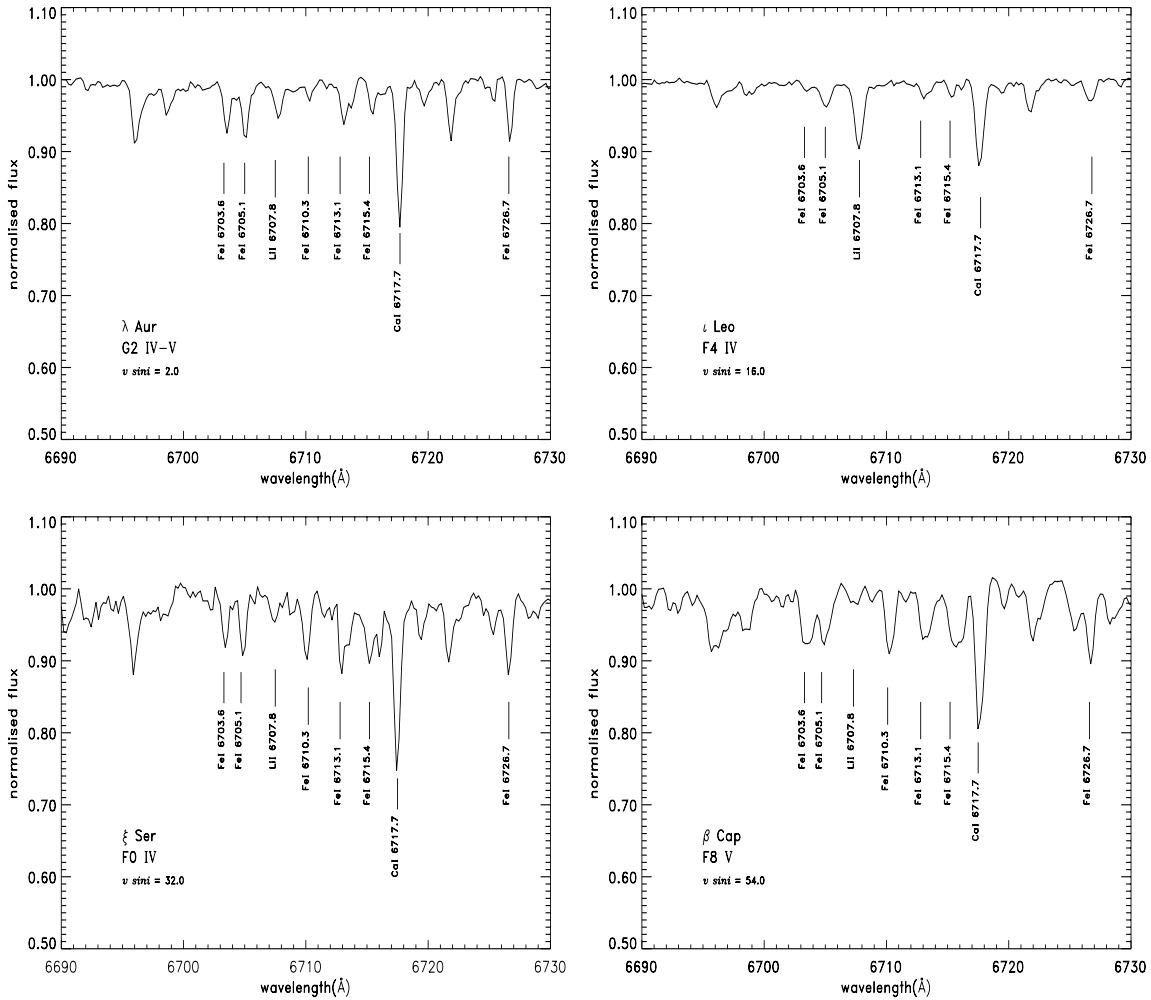


Fig. 1. A few normalised sample spectra in the neighbourhood of the Li I 6707.8 Å line. Note the fairly strong Li line in ι Leo and relatively weak in the other three stars.

excitation potential as the 6707.445 Å Fe I blend. Using MOOG (the standard LTE line analysis code due to Sneden 1973, upgraded 2001) and the model atmospheres of Gustafsson et al. (1975, upgraded 1992) with the grid generated by Luck (1992), Fe abundances were calculated for these lines with the appropriate line data and the observed EQWs as the input. The EQW of the Fe I (6707.445 Å) blend in the Li feature was then estimated using MOOG, the same model atmosphere and the Fe abundance determined above. The average of the EQWs thus obtained was adopted as the strength of the Fe I blend and subtracted from the measured EQW of the Li feature to yield the EQW of the Li I component alone. The EQWs of the blended feature (LiI + FeI), Fe I and Li I are tabulated in Cols. 12–14 respectively. With these corrected Li EQWs as the input and an appropriate choice of the models based on the stellar parameters from the grid of model atmospheres, Li abundances have been determined again using MOOG. For stars rotating more rapidly than 35 km s^{-1} , Li abundances were determined by fitting synthetic spectra to the observed using $v \sin i$ and $\log N(\text{Li})$ as free parameters. The Li EQW quoted for these in the table have been calculated from these synthetic fits. All these abundances have been determined by treating the Li feature as a blend of two lines with

gf values of 0.989 and 0.494. These are given in Col. 15. Only upper limits to the Li abundances could be given for stars for which $v \sin i$ is too large and/or the Li line is too weak for the Li EQW to be measured accurately.

The Li abundance depends strongly and almost exclusively on T_{eff} . It is very important to use a uniform temperature scale for any meaningful comparison of Li abundances. T_{eff} in the present study has been derived from the recent $T_{\text{eff}} - (B - V)$ calibration of Flower (1996) and are tabulated in Col. 4. A change in T_{eff} of 200 K changes the Li abundance by a substantial amount of 0.22 to 0.30. However, the Li abundance is very insensitive to changes in gravity. A change of ± 0.25 in the gravity changes it by 0.01 to 0.03. It changes by an equal amount for a change of ± 0.5 in ξ_t . The dependence on metallicity of the model is even more negligible. An error in EQW of 5 mÅ leads to a larger change in $\log N(\text{Li})$ for stars with lower Li I EQW e.g., a change of 0.18 for EQW of 15 mÅ. The same error for a star with high Li I EQW of 115 mÅ yields a change in $\log N(\text{Li})$ of only 0.05. Accounting for uncertainties arising from T_{eff} , ξ_t and $\log g$, the accuracy in the determination of $\log N(\text{Li})$ is expected to be within ± 0.2 to ± 0.25 dex, given the error in the EQW measurement. The Hipparcos Catalogue contains astrometric data providing parallaxes with precision of around a

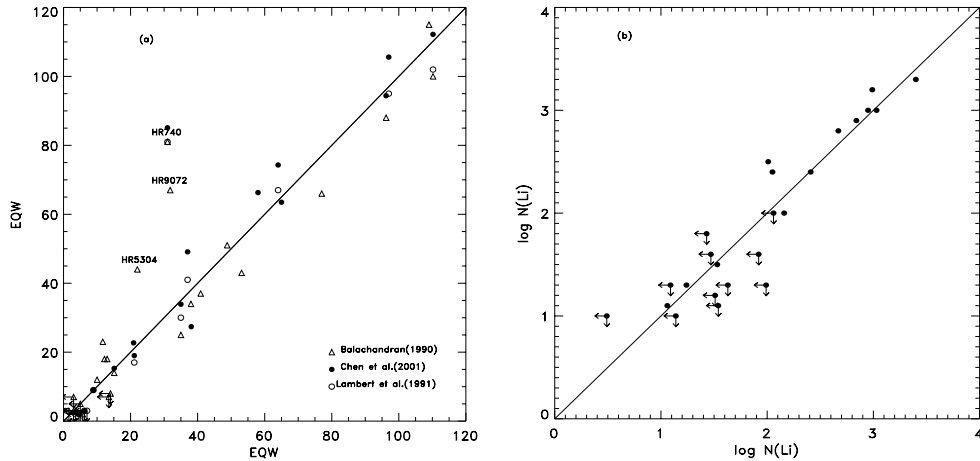


Fig. 2. **a)** Equivalent widths compared with those of other studies. Symbols are described in the key. **b)** Li abundance compared with that of Lebre et al. (1999). Arrows pointing left and downwards mark upper limits to Li abundance.

milliarcsec and photometric data giving apparent visual magnitude with a precision of ~ 0.002 mag enabling an estimate of distances to an accuracy of better than 10 per cent. From these data the absolute visual magnitudes for all the above stars have been estimated and using the bolometric corrections of Flower (1996), luminosities obtained and they are listed in Col. 9 of Table 1. The error in $\log L/L_{\odot}$ is within ± 0.08 .

A number of our stars have been previously analyzed for their Li abundance. 26 out of the 127 stars are in common with Balachandran (1990), 16 in common with Chen et al. (2001), 11 in common with Lambert et al. (1991) and 23 in common with Lebre et al. (1999). Figure 2a gives the plot of our EQWs vs. the EQWs of Balachandran (1990), Lambert et al. (1991) and Chen et al. (2001). The symbols are described in the figure. A 45° line cuts through the points. The arrows pointing downwards denote stars with upper limits. The most glaring discrepancy is noted in HR 740 which in all the other 3 studies is measured to have EQW close to $80 \text{ m}\text{\AA}$. We have rechecked and remeasured and our measurement of it in no way exceeds $30 \text{ m}\text{\AA}$. The other 2 quite discrepant points are those of HR 5304 and HR 9072 which differ from those of Balachandran (1990). The agreement among the rest of the stars is quite good; it is within the limits of the accuracy of the Li abundance determination. Lebre et al. (1999) do not list EQWs for their stars, so we have plotted their $\log N(\text{Li})$ vs. ours in Fig. 2b. The agreement is pretty good considering many of the stars in the lower half have upper limits to Li abundance, so they could be tending towards the 45° line.

3. Interpretation and implications

3.1. Lithium abundance trends with temperature and metallicity

The plot between $\log N(\text{Li})$ and T_{eff} (Fig. 3a) shows a gradual decrease in $\log N(\text{Li})$ towards lower T_{eff} with a rather sharp drop at $\sim 5300 \text{ K}$ which marks the onset of dilution on the subgiant branch. No subgiants cooler than this show high Li and the hotter ones present a large dispersion in $\log N(\text{Li})$ for similar T_{eff} implying that depletion has indeed already occurred on

the MS. Stars with upper limits to Li abundance are denoted by inverted triangles. Part of the reason why they also display a linear correlation between $\log N(\text{Li})$ and T_{eff} is the observational detection limit, a constant measurable EQW limit which leads to larger abundances at higher temperatures.

The stars above include stars that have evolved out of the “Li-dip” on the main sequence in the temperature interval $6500\text{--}6800 \text{ K}$. One could deduce from the theoretical tracks plotted on the HR diagram as they evolve from the ZAMS that this temperature range on the MS corresponds to mass range roughly between 1.2 and $1.35 M_{\odot}$. Balachandran (1990) and Chen et al. (2001) have noted that the Li dip does not occur at the same mass at all metallicities, i.e. the mass of the Li-dip stars is dependent upon metallicity; it is at a lower mass for the more metal-poor stars. For the metallicity range covered in the present study, it is adequate to assume Li-dip stars fall within $1.15\text{--}1.4 M/M_{\odot}$. Even when these stars are excluded from Fig. 3a as done in Fig. 3b, we note that it does not alter the behaviour of $\log N(\text{Li})$ with T_{eff} . The effect of the dip is not so obvious. Stars with large depletions are scattered through the entire temperature range. The large Li spread to the left of $T_{\text{eff}} = 5300 \text{ K}$ persists almost over the entire temperature range observed. The Li-dip stars corresponding to $1.15\text{--}1.4 M_{\odot}$ incidentally are spread over temperature range roughly between 5900 and 6900 K after they have evolved from the MS. Figure 3c shows the Li abundance of the Li-dip stars plotted against T_{eff} .

Figure 4a shows a plot of $\log N(\text{Li})$ against T_{eff} for various metallicities. The filled symbols are upper limits to Li abundance. A close inspection, despite the large scatter at a given T_{eff} , does suggest higher $\log N(\text{Li})$ for higher metallicities. This is discerned better in Fig. 4b where $\log N(\text{Li})$ is plotted against $[\text{Fe}/\text{H}]$ ranging from -0.85 to $+0.75$. Rebolo et al. (1988), Lambert et al. (1991) and recently Chen et al. (2001) have done a detailed study of Li abundance as a function of $[\text{Fe}/\text{H}]$ over a large range and find that the upper envelope of the distribution of stars increases from $\log N(\text{Li}) \sim 2.2$ at $[\text{Fe}/\text{H}] \sim -1.4$ to about 3.3 at $[\text{Fe}/\text{H}] \sim 0.0$ with a spread in Li abundance at a given metallicity that increases with

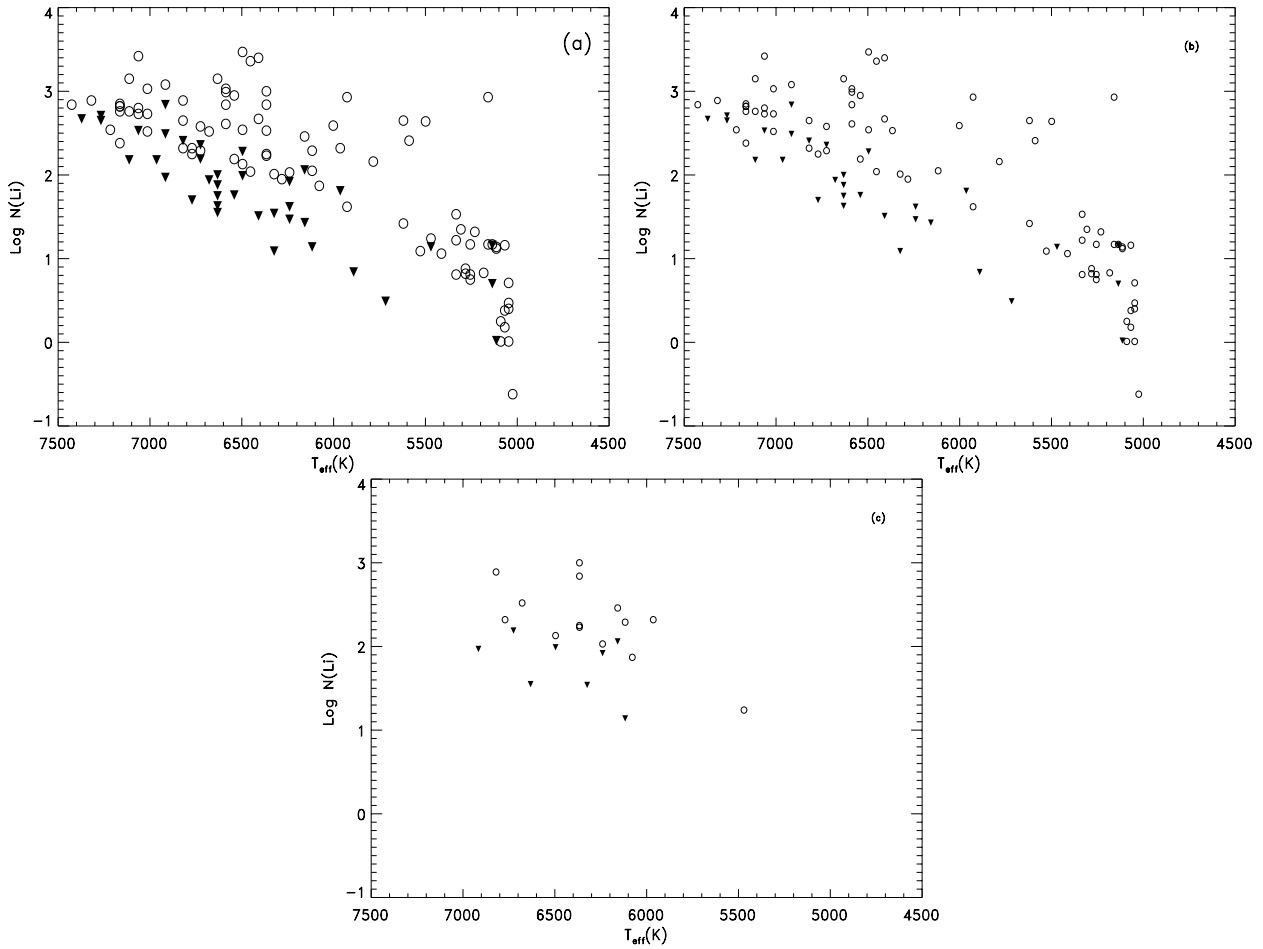


Fig. 3. Lithium abundance vs. effective temperature **a)** for the entire sample. **b)** For the sample exclusive of Li-dip stars. **c)** For only the Li-dip stars. Inverted triangles denote upper limits to Li abundance.

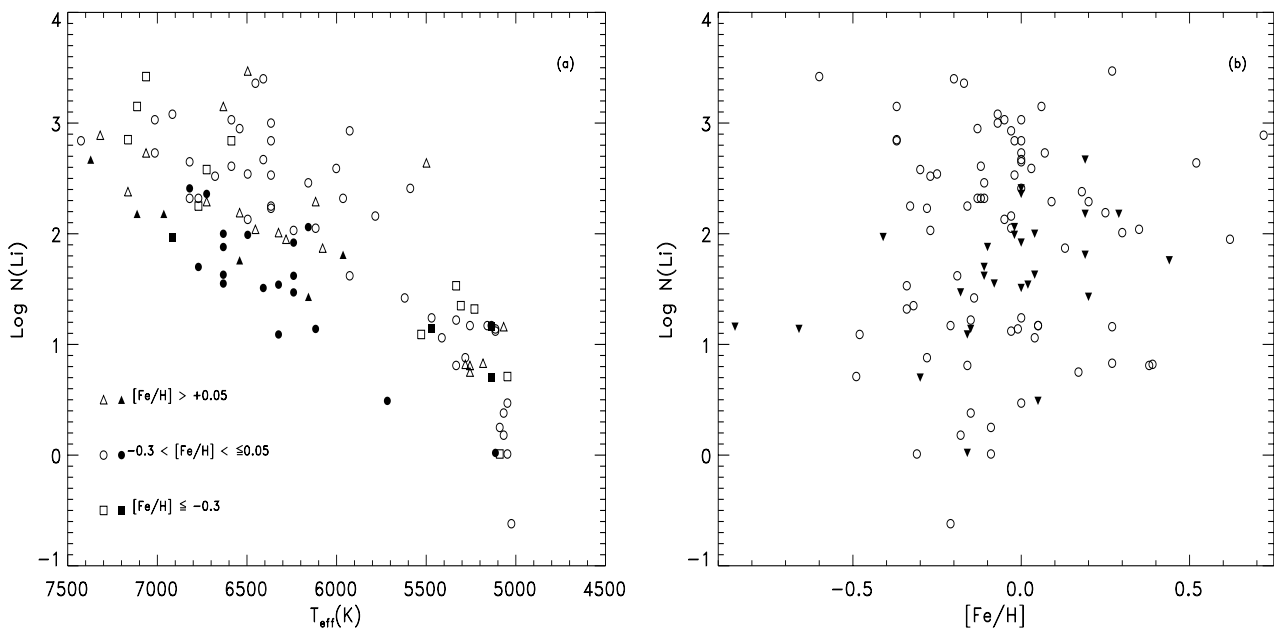


Fig. 4. **a)** Li abundance vs. T_{eff} for various [Fe/H] bins defined in the key. The filled symbols are upper limits to Li abundance. **b)** Li abundance vs. [Fe/H] for the entire sample. Inverted triangles denote upper limits to Li abundance.

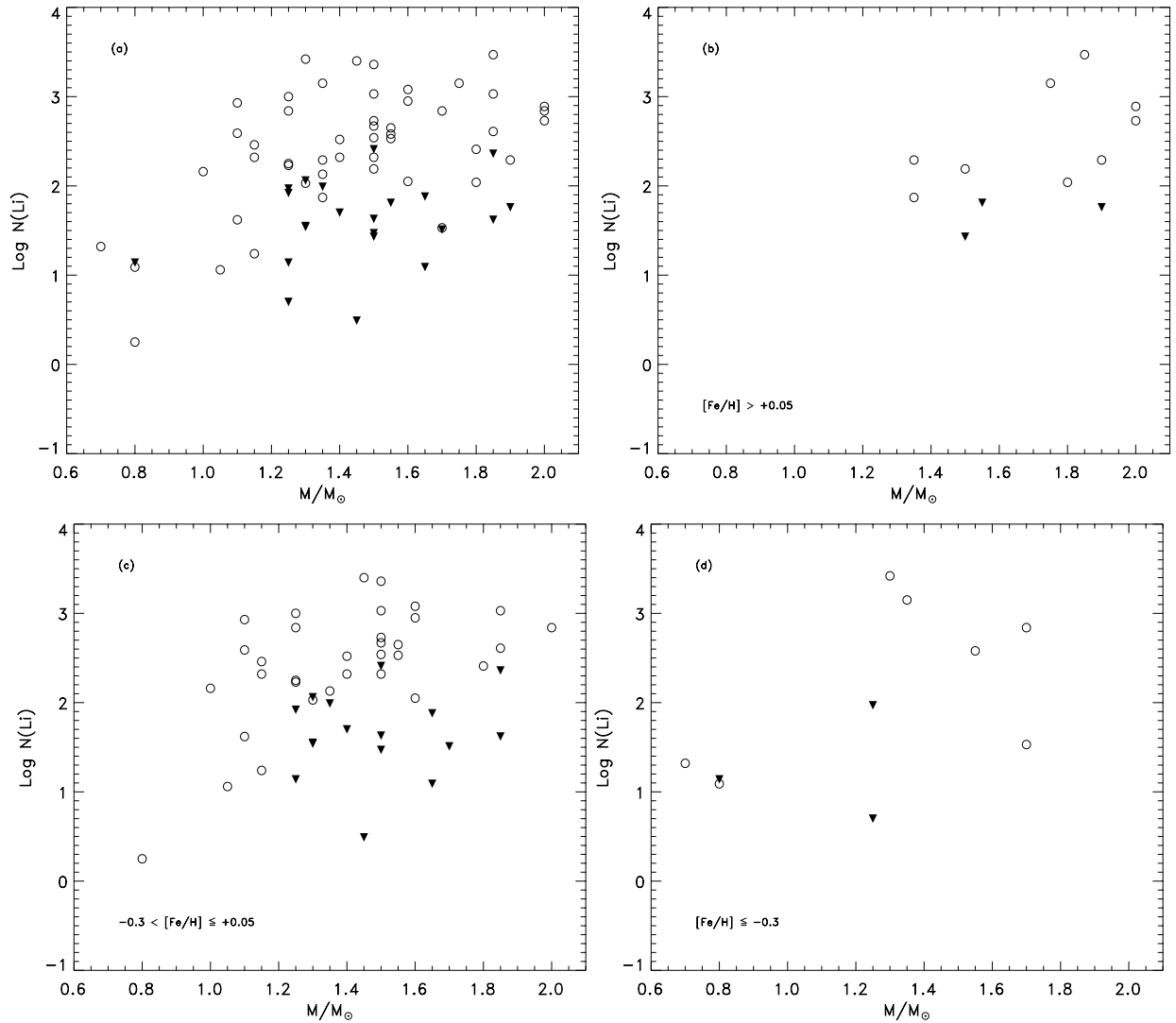


Fig. 5. Li abundance vs. stellar mass **a)** for the entire sample up to $2.0 M_{\odot}$ **b)** for the same sample for $[\text{Fe}/\text{H}] > +0.05$ **c)** for $-0.3 < [\text{Fe}/\text{H}] \leq +0.05$ **d)** for $[\text{Fe}/\text{H}] \leq -0.3$. The inverted triangles denote stars with upper limits to lithium abundance.

increasing metallicity. The present survey demonstrates a very similar trend over the $[\text{Fe}/\text{H}]$ span in common with theirs with a similarly large spread in Li abundance at any given $[\text{Fe}/\text{H}]$. It is important to understand why there is large dispersion in $\log N(\text{Li})$ at a given $[\text{Fe}/\text{H}]$, especially for higher metallicities.

3.2. Lithium abundance trends with mass and age

Since the mass of a star is its basic underlying property that determines, for example, the depth of the convection zone of the star, it is worth investigating how Li abundances could be related to mass. The mass of each star of our sample was derived using the set of evolutionary tracks appropriate to its metallicity. For stars of $[\text{Fe}/\text{H}] \leq -0.3$ and $>+0.05$, the $Z = 0.008$ and $Z = 0.03$ tracks were used respectively; for stars in the range $-0.3 < [\text{Fe}/\text{H}] \leq 0.05$, the $Z = 0.019$ tracks were used (Girardi et al. 2000). Masses thus estimated are displayed in Col. 10 of Table 1. Figure 5a plots $\log N(\text{Li})$ for stars in the mass range 0.5 – $2.0 M_{\odot}$. There is a distinctly clear trend of Li abundance increasing with mass. Figures 5b–d show the

same for different metallicities. However, it is accompanied by a dispersion much too large to be explained by metallicity or age. Age of each star was determined from the set of theoretical isochrones of Girardi et al. (2000) appropriate to its metallicity and is tabulated in Col. 11 of Table 1. Figure 6 shows the plot between $\log N(\text{Li})$ and T_{eff} with each star marked by its age in Gyrs. It demonstrates clearly that while the Li spread partly owes itself to the spread in age of stars, there are also several stars of similar ages at any given T_{eff} and yet have different amounts of depletion of Li. This further reiterates the fact that there are variables other than mass, age and metallicity playing a role in describing the observed patterns of Li abundance.

3.3. Lithium abundance and $v \sin i$

The present study in F and G subgiants has been especially undertaken to explore the effect of one such variable, i.e., rotation on the depletion of Li. The projected rotational velocity $v \sin i$ for all the stars is plotted vs. T_{eff} in Fig. 7. This plot shows the well known sharp cut off around 6400 K to the right of which

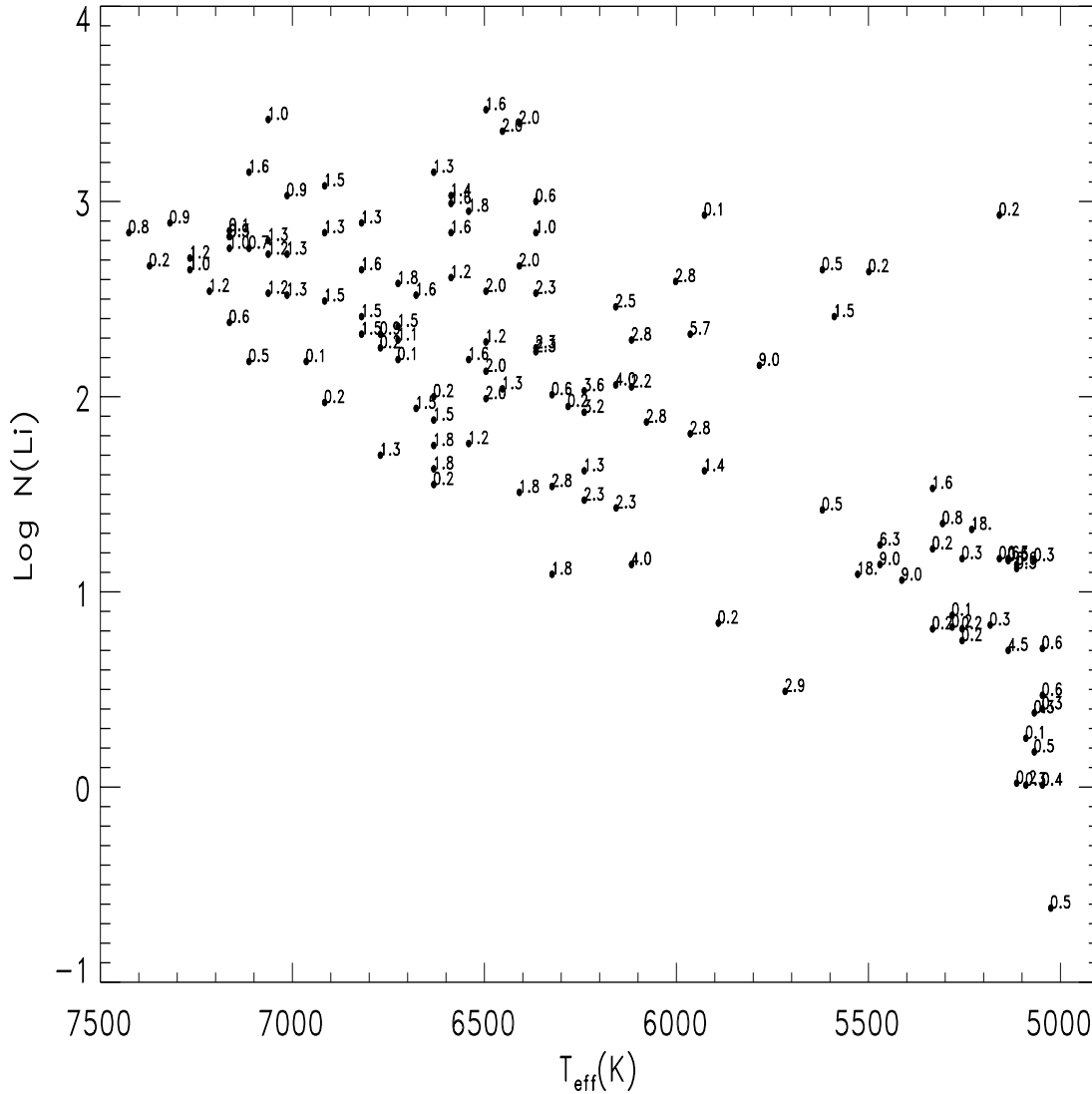


Fig. 6. Li abundance vs. T_{eff} for the entire sample. Marked on the diagram is the age for each star in Gyrs.

all stars have spun down to low values ($v \sin i \leq 20 \text{ km s}^{-1}$) and stars to the left of it have a large spread in $v \sin i$ ranging from 2 to higher than 100 km s^{-1} . So the stars in the temperature range 5300–6400 K exhibiting a large spread in Li (as seen in Figs. 3a and b) have already spun down to low values of $v \sin i$. On the other hand, stars to the left of the rotational drop more or less preserve their intrinsic range in rotational velocity primarily because of their thinner convective envelopes.

Figures 8a and b display the relationship between Li abundance and $v \sin i$ respectively for stars inclusive of the Li-dip ones and for stars without them. Both the figures suggest that although there is a large dispersion in $\log N(\text{Li})$ at small $v \sin i$, the Li-depleted stars tend to be concentrated only at these low values of $v \sin i$. None of them exist at large $v \sin i$. On the other hand, rapidly rotating stars tend to retain undepleted values of Li abundance. This trend seems to suggest that stars which are still fast rotators, (so no differential rotation has set in) have obviously lost little angular momentum and have therefore suffered little mixing and Li depletion. On the other hand, among the slowly rotating stars, stars that were born slow

rotators have the same story to tell but those which were born fast rotators have suffered much larger angular momentum loss and have consequently undergone much more effective mixing and hence greater Li depletion. This implies that Li depletion depends upon the magnitude of the change in rotational velocity of a star, i.e., from what it was initially endowed with to its present value. In this scenario, a group of stars that arrive on the MS with the same cosmic Li abundance and a large range in rotational velocity will be seen to exhibit a large range in Li abundance after they have all spun down. The plot between $\log N(\text{Li})$ and $v \sin i$ arranged according to different $(B - V)$ bins is shown in Fig. 8c. It demonstrates beautifully that the higher temperature stars have retained more or less their initial Li abundance over the entire range of $v \sin i$. These are the early F stars with thinner convective envelopes which more or less preserve their intrinsic range of rotational velocity; as a consequence have lost little angular momentum, therefore hardly any Li depleted. On the other hand, lower temperature stars have all spun down and show a large spread in Li but concentrated towards depleted values of

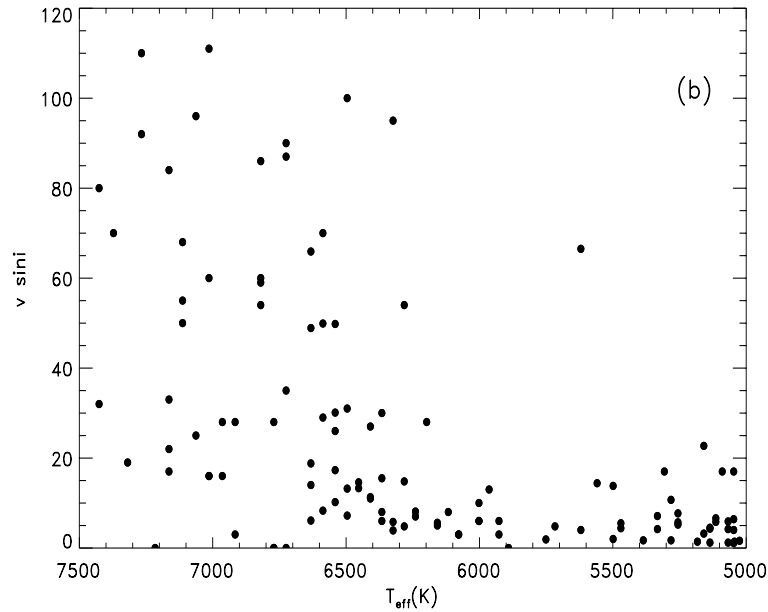


Fig. 7. $v \sin i$ vs. effective temperature for stars of Table 1.

Li, the amount of depletion directly depending upon the magnitude of the change in rotational velocity. There is no one-to-one correlation between Li abundance and the present projected rotational velocity. Instead, the above trend seems to be driven by the rotational history of the star. However, it is extremely important to note here that though the upper boundary in Fig. 8 is almost independent of $v \sin i$, the lower envelope running from high Li and high $v \sin i$ to low Li and low $v \sin i$ appears to skirt stars with upper limits to Li abundance denoted by inverted triangles in Figs. 8a and b. This could arise because the minimum detectable EQW limit of the Li line, set by the spectrum quality increases with increasing $v \sin i$. So the lower envelope may just be an artifact of this inherent limitation of the Li EQW measurement for large $v \sin i$. If this is indeed true, then the interpretation based on Fig. 8 needs to be modified.

3.4. Lithium evolution on the HR diagram

Nevertheless, it is interesting to further explore how the Li abundance of stars evolves as a function of mass, age and rotation when plotted on the HR diagram against the backdrop of the theoretical evolutionary tracks. Figure 9 displays the tracks due to Girardi et al. (2000) for masses ranging from 0.8 to 7 M_{\odot} for a typical Pop. I composition: $Z = 0.019$ and $Y = 0.273$. The increasing size of the symbols denotes increasing $v \sin i$. Stars are broken up into 2 Li abundance bins. The open circles are stars with $\log N(\text{Li}) \geq 2.0$ and filled circles with $\log N(\text{Li}) < 2.0$. The 6 bins A to F are described in the key. Stars in bins A, B and C are divided down the HR diagram with the fastest rotators being the most massive stars and the slowly rotating stars the least massive. This is also true for bins D, E and F. The lower mass stars have already spun down to $v \sin i \leq 20 \text{ km s}^{-1}$ while the more massive stars do so towards the end of the subgiant branch where they are dominated by the depleted values of Li abundance due to

dilution. To the left of $\log T_{\text{eff}} = 3.8$ where the rotational discontinuity occurs, stars of $M \geq 1.4 M_{\odot}$ tend to have a large range in $v \sin i$ and higher Li. Early F stars because of their thinner convective envelopes are expected to experience little loss of angular momentum and therefore hardly any mixing and depletion of Li. On the other hand, stars of $M < 1.4 M_{\odot}$ (late F stars with deeper convective envelopes) have undergone much larger losses of angular momentum and have a preponderance of lower Li values.

This entire sample of stars is plotted on the HR diagram in Fig. 10, now with symbol size indicating Li abundance. It is worth emphasizing that in the present survey, Li-dip stars that lie in the mass range 1.15–1.4 M_{\odot} are not all upper limits, contrary to what is noted by Balachandran (1990) and Chen et al. (2001). Li-dip stars are not necessarily stars with $\log N(\text{Li}) \leq 2.0$ and the upper limits are stars not all with $\log N(\text{Li}) \leq 2.0$. It is interesting to note though that as we move across the HR diagram from higher masses, the Li abundance does drop in the region identified as that of the dip and rises again in the lower mass stars which also include those which are depleted severely owing to deeper convective zone for lower masses. It is clear, however, that stars in 1.2–1.35 M_{\odot} range which appear to have evolved from MS effective temperatures between 6500–6800 K, i.e. the Li-dip stars indeed show depleted values of Li.

A comparison of Figs. 9 and 10 distinctly confirms the trend that there is a large spread in $\log N(\text{Li})$ for stars of low $v \sin i$ for all masses whereas stars of high $v \sin i$ and larger masses tend to have only higher values of Li. This reiterates what is apparent in Figs. 8a–c that the large Li spread observed in these stars owes itself to the change in the rotational velocity of a star from what it was initially endowed with to its present value. Very recently, Reiners & Schmitt (2003) have obtained high resolution ($R \sim 220\,000$) spectra of 144 dwarfs of spectral types F–K and precisely determined rotational velocities using the Fourier Transform Method. For stars with $v \sin i \geq 10 \text{ km s}^{-1}$ it is

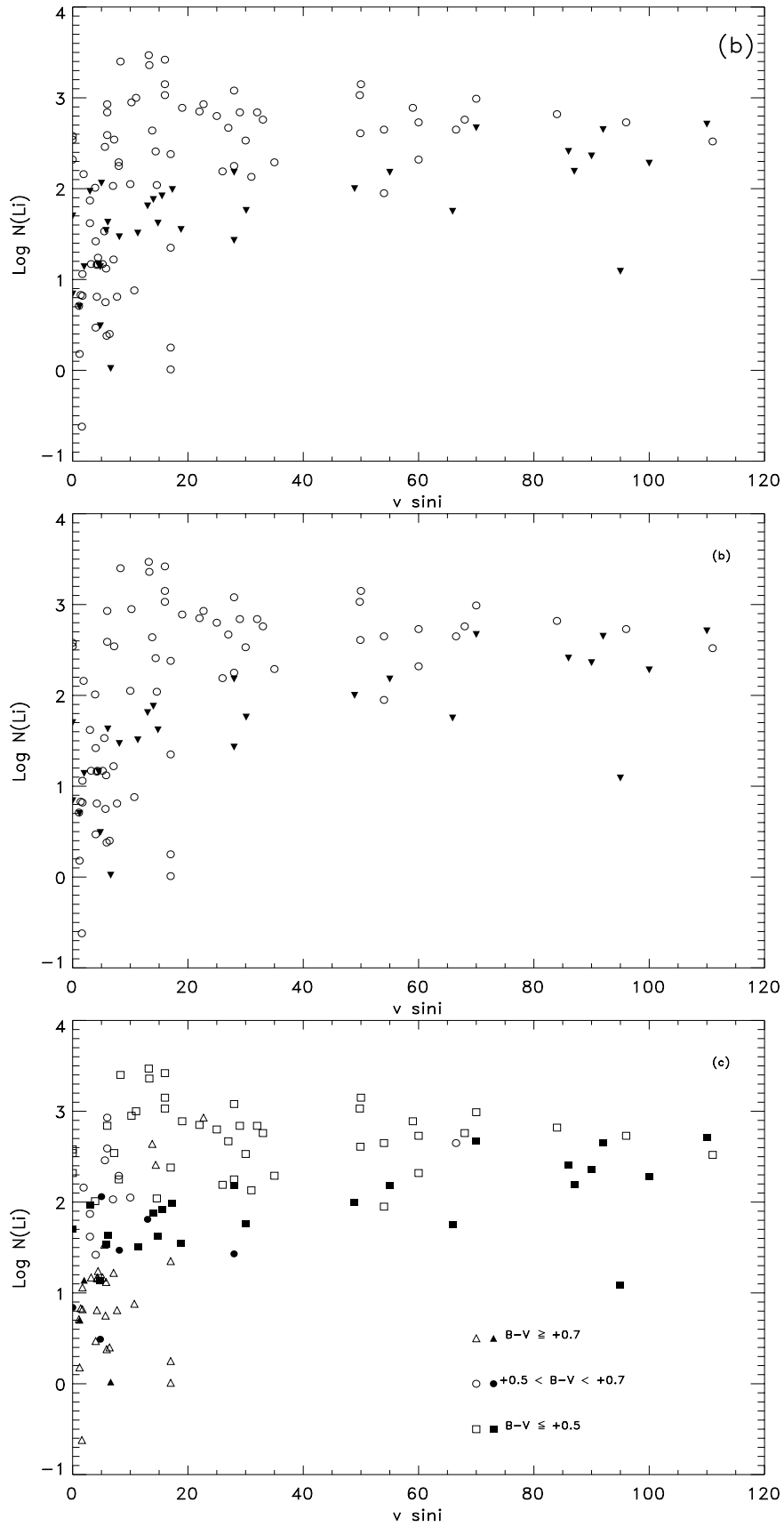


Fig. 8. Lithium abundance vs. $v \sin i$ **a)** For stars of Table 1. **b)** For the sample excluding Li-dip stars. Inverted triangles denote stars with upper limits to lithium abundance. **c)** For the entire sample with various $(B - V)$ bins. The filled symbols are stars with upper limits.

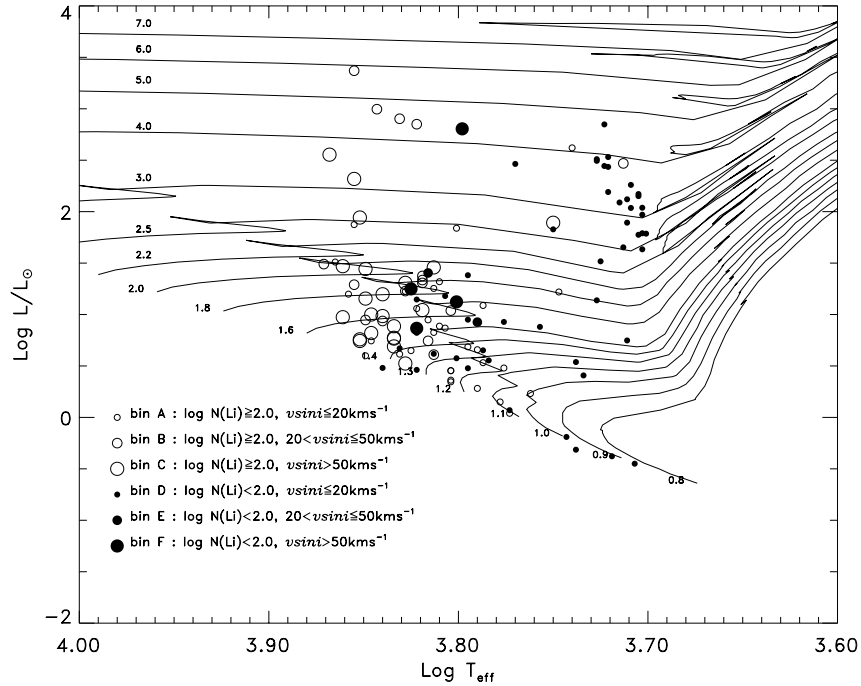


Fig. 9. HR diagram of the observed stars for which absolute visual magnitudes are determined from the Hipparcos data. Symbols of increasing size denote increasing $v \sin i$. Unfilled circles denote $\log N(\text{Li}) \geq 2.0$ while the filled ones denote $\log N(\text{Li}) < 2.0$. The bins chosen are indicated in the key. Also shown are theoretical evolutionary tracks of Girardi et al. (2000) for stars of masses ranging from 0.8 to 7.0 M_{\odot} for Pop. I composition: $Z = 0.019$, $Y = 0.273$.

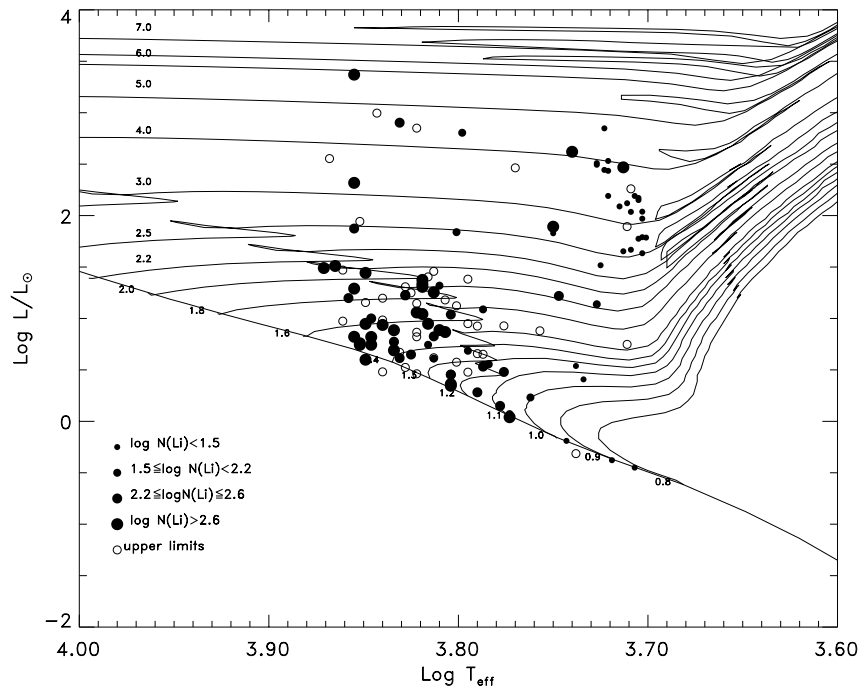


Fig. 10. The entire sample plotted on the HR diagram. The ZAMS and the evolutionary tracks are due to Girardi et al. (2000) for a Pop. I composition. Each track is labelled in solar masses. The size of the filled circle upper limits.

possible to measure differential rotation using this method and in about 25% of them they have been able to do so. Interestingly they find that Li-depleted stars turn out to show strong signatures of differential rotation. We have 4 stars in common with theirs, namely, HR 4054, HR 5185, HR 5235 and HR 5338 out of the 18 stars for which their measurements support the idea

that Li depletion is closely connected to differential rotation. This by no means implies that mixing induced by differential rotation is the only viable mechanism accounting for depletion of Li in stars otherwise similar. The aim of our study of Li depletion in F and early G subgiants was primarily to attempt to investigate whether our observations support such an idea.

As Pasquini (2000) has highlighted, it is not easy to assess the role of rotation because the driving parameter is expected to be the rotational history of the star and not the present, measured $v \sin i$ value. Apart from the fact the lower envelope in Figs. 8a–c might actually have no physical basis and increasing the sample of stars even by an order of magnitude might not change this, there are at least 3 observations in the recent past that don't seem to support the angular momentum and material transport via turbulence. An important prediction of this model is that short-period tidally-locked binaries with different rotational histories than single stars of the same age and mass should show significantly larger Li abundances. Balachandran (2002, private communication) has examined these in the Hyades and M 67 clusters and found that the Li abundances are entirely compatible with what is expected from single stars. Secondly, the above model requires a star to have a rapidly rotating core. Helioseismology has revealed that the present-day Sun down to $r = 0.2 R_{\odot}$ is already rotating slowly as a rigid body. So the angular momentum transport and dissipation have been far more efficient than predicted by this model. Lastly, another prediction of this model is a slow, deep mixing occurring inside the star which then should also deplete Be which burns at 3.5×10^6 K. However, there is no depletion of Be in the Sun. A simultaneous measurement of Be and Li in stars is likely to pin down the nature of mixing processes operating inside them. The Be II lines at 3130 Å are near the atmospheric UV cut-off. The lines are in a crowded region of the spectrum and the blending is severe. Observations of these are not easy but there have been several recent studies of these lines in a sample of F and G field dwarfs as well as Hyades dwarfs (Garcia Lopez et al. 1995; Deliyannis et al. 1998; Boesgaard et al. 2001; Boesgaard & King 2002). Although the depletion in Be is clearly observed in the Li dip stars, there is little to no depletion in cooler stars. From Boesgaard & King's (2002) observations of 34 F and G dwarfs in the Hyades, there is strong evidence of a Be dip in the F stars where the Li drop occurs. The Li and Be abundances are not just correlated but are occurring together in this temperature range. They find good agreement with the rotational mixing calculations of Deliyannis & Pinsonneault (1997). Be observations of a large sample of F and G stars are in order to ascertain the role of rotation-induced mixing process in stars other than in the Li Dip.

References

- Balachandran, S. 1990, *ApJ*, 354, 310
 Balachandran, S. C. 1995, *ApJ*, 446, 203
 Balachandran, S. C. 2002, private communication
 Balachandran, S., Lambert, D. L., & Stauffer, J. R. 1988, *ApJ*, 333, 267
 Balachandran, S., Lambert, D. L., & Stauffer, J. R. 1996, *ApJ*, 470, 1243
 Boesgaard, A. M., Deliyannis, C. P., King, J. R., & Stephens, A. 2001, *ApJ*, 553, 754
 Boesgaard, A. M., & King, J. R. 2002, *ApJ*, 565, 587
 Boesgaard, A. M., & Tripicco, M. J. 1986, *ApJ*, 302, L49
 Cayrel de Strobel, G., Soubiran, C., Friel, E. D., Ralite, N., & Francois, P. 1997, *A&AS*, 124, 299
 Charbonnel, C., Vauclair, S., Maeder, A., Meynet, G., & Shaller, G. 1994, *A&A*, 283, 155
 Chen, Y. Q., Nissen, P. E., Benoni, T., & Zhao, G. 2001, *A&A*, 371, 943
 De Medeiros, J. R., do Nascimento, J. D., Jr., & Mayor, M. 1997, *A&A*, 317, 701
 De Medeiros, J. R., & Mayor, M. 1999, *A&AS*, 139, 443
 Deliyannis, C. P. 2000, in *Stellar Clusters and Associations: Convection, Rotation and Dynamos*, ed. R. Pallavicini, G. Micela, & S. Sciortino, ASPCS, 198, 235
 Deliyannis, C. P., & Pinsonneault, M. H. 1997, *ApJ*, 488, 836
 Deliyannis, C. P., Boesgaard, A. M., Stephens, A., et al. 1998, *ApJ*, 498, L147
 Deliyannis, C. P., Pinsonneault, M. H., & Charbonnel, C. 2000, in *The Light Elements and their Evolution*, ed. L. da Silva, M. Spite, & J. R. de Medeiros (Astronomical Society of the Pacific), IAU Symp., 198, 61
 Duncan, D. K. 1981, *ApJ*, 248, 651
 ESA 1997, *The Hipparcos & Tycho Catalogues*, ESA SP-1200
 Flower, P. J. 1996, *ApJ*, 469, 355
 Garcia Lopez, R. J., Rebolo, R., & Perez de Taoro, M. R. 1995, *A&A*, 302, 184
 Girardi, L., Bressan, A., Bertelli, G., & Chiosi, C. 2000, *A&AS*, 141, 371
 Gustafsson, B., Bell, R. A., Eriksson, K., & Nordlund, Å. 1975, *A&A*, 42, 407
 Herbig, G. H. 1965, *ApJ*, 141, 588
 Hoffleit, D., & Jaschek, C. 1982, *The Bright Star Catalogue*, Fourth revised edition (New Haven, Connecticut: Yale University Observatory)
 Jeffries, R. D. 2000, in *Stellar Clusters and Associations: Convection, Rotation and Dynamos*, ed. R. Pallavicini, G. Micela, & S. Sciortino, ASPCS, 198, 245
 Jones, B. F., Fischer, D., Shetrone, M., & Soderblom, D. R. 1997, *AJ*, 114, 352
 Lambert, D. L., Heath, J. E., & Edvardsson, B. 1991, *MNRAS*, 253, 610
 Lebre, A., de Laverny, P., de Medeiros, J. R., Charbonnel, C., & da Silva, L. 1999, *A&A*, 345, 936
 Luck, R. E. 1992, private communication
 Mallik, S. V. 1998, *A&A*, 338, 623
 Pasquini, L., Liu, Q., & Pallavicini, R. 1994, *A&A*, 287, 191
 Pasquini, L., Randich, S., & Pallavicini, R. 1997, *A&A*, 325, 535
 Pasquini, L. 2000, in *The Light Elements and their Evolution*, ed. L. da Silva, M. Spite, & J. R. de Medeiros (Astronomical Society of the Pacific), IAU Symp., 198, 269
 Pinsonneault, M. H., Kawaler, S. D., Sofia, S., & Demarque, P. 1989, *ApJ*, 338, 424
 Pinsonneault, M. H., Kawaler, S. D., & Demarque, P. 1990, *ApJS*, 74, 501
 Randich, S., Gratton, R., & Pallavicini, R. 1993, *A&A*, 273, 194
 Randich, S., Giampapa, M. S., & Pallavicini, R. 1994, *A&A*, 283, 893
 Randich, S., Gratton, R., Pallavicini, R., Pasquini, L., & Caretta, E. 1999, *A&A*, 348, 487
 Randich, S., Pallavicini, R., Pasquini, L., & Gratton, R. 1995, *Mem. Soc. Astron. It.*, 66, 387
 Rebolo, R., Molaro, P., & Beckman, J. E. 1988, *A&A*, 192, 192
 Reiners, A., & Schmitt, J. H. M. M. 2003, *A&A*, 398, 647
 Snenen, C. A. 1973, Ph.D. Thesis, The University of Texas, Austin
 Soderblom, D. R., Jones, B. F., Balachandran, S., et al. 1993a, *AJ*, 106, 1059
 Soderblom, D. R., Fedele, S. B., Jones, B. F., Stauffer, J. R., & Prosser, C. F. 1993b, *AJ*, 106, 1080
 Thorburn, J. A., Hobbs, L. M., Deliyannis, C. P., & Pinsonneault, M. H. 1993, *ApJ*, 415, 150